

Nucleon axial charge and the lowest moments of dimension-four operators from lattice QCD

Konstantin Ottnad

Nucleon Spin Structure at Low Q: A Hyperfine View

ECT* Trento, July 4th, 2018

JOHANNES GUTENBERG
UNIVERSITÄT MAINZ



Outline

① Introduction

- Operators, matrix elements, form factor decompositions

② Lattice Setup

- Ensembles
- Computational details, renormalization ...

③ Excited States

- Generalized pencil of functions
- **Simultaneous multi-state fit models**

④ Results + chiral and continuum extrapolations

In collaboration with:

Tim Harris, Harvey Meyer, Georg von Hippel, Jonas Wilhelm, Hartmut Wittig

Introduction

We consider nucleon forward matrix elements

$$\langle N(p', s') | \mathcal{O} | N(p, s) \rangle. \quad (1)$$

“Standard” nucleon charges (g_A , g_T , g_S) require **local** operators: $\mathcal{O} = \bar{q}\gamma_\mu\gamma_5 q$, $\bar{q}i\sigma_{\mu\nu}q$, $\bar{q}q$.

- Can be computed directly at zero momentum (unlike magnetic moment $\mu_N = G_M(0)$).
- Consider only observables with $Q^2 = 0$.

Nucleon quark momentum fraction is the first moment of unpolarized quark distribution:

$$\langle x \rangle_q = \int_0^1 x \cdot [q(x) + \bar{q}(x)]. \quad (2)$$

Similarly: First momenta for **helicity** (Δq) and **transversity** (δq) distributions.

On the lattice they require one-derivative, **dimension-four** operators:

$$\mathcal{O}_{\mu\nu}^{vD} = \bar{q}\gamma_{\{\mu} \overleftrightarrow{D}_{\nu\}} q, \quad \mathcal{O}_{\mu\nu}^{aD} = \bar{q}\gamma_{\{\mu} \gamma_5 \overleftrightarrow{D}_{\nu\}} q, \quad \mathcal{O}_{\mu\nu\rho}^{tD} = \bar{q}\sigma_{[\mu\{\nu} \overleftrightarrow{D}_{\rho\}} q, \quad (3)$$

where

- $\{\dots\}$ denotes symmetrization over indices and subtraction of the trace,
- $[\dots]$ denotes anti-symmetrization over indices.

Matrix elements, FF decomposition and ratios

Can compute forward nucleon matrix elements in lattice QCD, but extracting nucleon structure information requires additional steps:

- For e.g. $\mathcal{O}_{\mu\nu}^{vD}$ the FF decomposition of the nucleon matrix element reads

$$\begin{aligned} \langle N(p', s') | \mathcal{O}_{\mu\nu}^{vD} | N(p, s) \rangle = \bar{u}(p', s') & \left[\gamma_{\{\mu} \bar{P}_{\nu\}} A_{20}(Q^2) - \frac{\sigma_{\{\mu\alpha} Q_\alpha Q_{\nu\}}}{2m_N} B_{20}(Q^2) \right. \\ & \left. + \frac{1}{m_N} Q_{\{\mu} Q_{\nu\}} C_{20}(Q^2) \right] u(p, s). \end{aligned} \quad (4)$$

- Spin-projecting with $\Gamma_0 = \frac{1}{2}(1 + \gamma_0)$ and $\Gamma_z = \Gamma_0(1 + i\gamma_5\gamma_3)$ and considering zero momentum transfer $Q = 0$ we compute the ratio

$$R^{vD}(t_f, t, t_i) \equiv \frac{C_{3\text{pt}}^{\mu\mu}(\vec{q} = 0, t_f, t_i, t; \Gamma_z)}{C_{2\text{pt}}(\vec{q} = 0, t_f - t_i; \Gamma_0)} \rightarrow \begin{cases} -\frac{3}{4}m \langle x \rangle_{u\pm d} & \text{for } \mu = 0 \\ +\frac{1}{4}m \langle x \rangle_{u\pm d} & \text{for } \mu = 1, 2, 3 \end{cases}, \quad (5)$$

for $t_f - t \gg 1$, $t - t_i \gg 1$ and where $\langle x \rangle_{u\pm d} \equiv A_{20}(0)$.

- In practice $t_{\text{sep}} \equiv t_f - t_i \lesssim 1.5 \text{ fm}$:

\Rightarrow Ground state convergence not guaranteed, fitting the ratio ("plateau method") not good enough...

Similar relations hold for $\mathcal{O}_{\mu\nu}^{aD}$, $\mathcal{O}_{\mu\nu\rho}^{tD}$: *Phys. Lett. B594 (2004) 164-170*

$$R^{aD}(t_f, t, t_i) \rightarrow -\frac{i}{2} m \langle x \rangle_{\pm u \Delta \pm d} \quad \text{for } \mu = 3, \nu = 0, \quad (6)$$

$$R^{tD}(t_f, t, t_i) \rightarrow +\frac{i}{4} m (2\delta_{0\rho} - \delta_{0\mu} - \delta_{0\nu}) \langle x \rangle_{\pm u \delta \pm d} \neq 0 \text{ for e.g. } \mu = 0, \nu = 1, \rho = 2. \quad (7)$$

and for the local operators.

g_A and $\langle x \rangle$ are closely related to the nucleon spin structure:

$$J_N = \sum_q \underbrace{\left(\frac{1}{2} \Delta q + L_q \right)}_{\equiv J_q} + J_g. \quad (8)$$

Phys. Rev. Lett. 78, 610 (1997)

- $\Delta q = g_A^q$ is the quark spin contribution.
- The total quark angular momentum J_q is related to the second Mellin-moment of the unpolarized nucleon PDF

$$J_q = \frac{1}{2} \left(A_{20}^q(0) + B_{20}^q(0) \right), \quad A_{20}^q(0) = \langle x \rangle_q. \quad (9)$$

- $B_{20}^q(0)$ cannot be obtained directly at $Q^2 = 0$; needs extrapolation of GFF data
- (Very) recent lattice results by ETMC (2017), PNDME (2018).
- This talk: focus on extraction of (isovector) g_A^{u-d} , $\langle x \rangle_{u-d}$ and **treatment of excited states**.

Computation of 2pt and 3pt functions

We use the truncated solver method:

$$\langle \mathcal{O} \rangle = \left\langle \frac{1}{N_{LP}} \sum_{i=1}^{N_{LP}} \mathcal{O}_n^{LP} \right\rangle + \langle \mathcal{O}_{\text{bias}} \rangle, \quad \mathcal{O}_{\text{bias}} = \frac{1}{N_{HP}} \sum_{i=1}^{N_{HP}} (\mathcal{O}_n^{HP} - \mathcal{O}_n^{LP}) \quad (10)$$

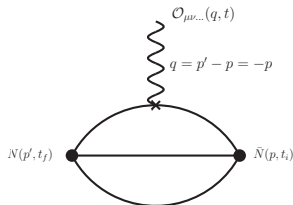
Comput. Phys. Commun. 181 (2010) 1570-1583
Phys. Rev. D91 (2015) no.11, 114511

Typically, per configuration:

- $N_{HP} = 1$ high-precision inversion(s)
- $N_{LP} = 16 \dots 48$ low-precision inversions

→ **Gain of factor 2-3 in compute time**

- For 3pt functions we use sequential inversions through the sink, setting $p' = 0$.
- **Isvector matrix elements require only quark-connected 3pt functions**
- For isoscalar matrix elements we work on adding disconnected diagrams



Lattice setup

To obtain physical results from lattice simulations one needs to:

- **Control discretization effects:**

- Simulate at different (small) values of the lattice spacing a .
- Perform continuum extrapolation.
- We have simulations at four values of a (0.049 fm, 0.064 fm, 0.076 fm and 0.086 fm).
- For some of the charges (g_A, g_S) exhibit only $\mathcal{O}(a^2)$ artifacts.

- **Correct for unphysical pion masses:**

- Simulate at several pion masses.
- Perform chiral extrapolation.
- Our pion masses range from ~ 200 MeV to ~ 350 MeV.
- We will add an ensemble with physical light quark mass.

- **Control finite size effects:**

- Simulate at large enough volumes.
- We use ensembles with $M_\pi L \gtrsim 4$.

Gauge ensembles

| ID | β | T/a | L/a | aM_π | M_π/GeV | $M_\pi L$ | N_{HP} | N_{LP} | twist-2 | t_{sep}/fm |
|------|---------|-----|-----|------------|--------------------|-----------|-----------------|-----------------|---------|----------------------------|
| C101 | 3.40 | 96 | 48 | 0.0976(09) | 0.223(3) | 4.68 | 1908 | 15264 | no | 1.0, 1.2, 1.4 |
| H102 | 3.40 | 96 | 32 | 0.1541(06) | 0.352(4) | 4.93 | 7988 | 0 | no | 1.0, 1.2, 1.4 |
| H105 | 3.40 | 96 | 32 | 0.1219(10) | 0.278(4) | 3.90 | 4076 | 48912 | yes | 1.0, 1.2, 1.4 |
| N401 | 3.46 | 128 | 48 | 0.1118(06) | 0.289(4) | 5.37 | 701 | 11216 | yes | 1.1, 1.2, 1.4, 1.5, 1.7 |
| S400 | 3.46 | 128 | 32 | 0.1352(06) | 0.350(4) | 4.33 | 1725 | 27600 | yes | 1.1, 1.2, 1.4, 1.5, 1.7 |
| D200 | 3.55 | 128 | 64 | 0.0661(03) | 0.203(3) | 4.23 | 1021 | 32672 | yes | 1.0, 1.2, 1.3, 1.4 |
| N200 | 3.55 | 128 | 48 | 0.0920(03) | 0.283(3) | 4.42 | 1697 | 20364 | yes | 1.0, 1.2, 1.3, 1.4 |
| N203 | 3.55 | 128 | 48 | 0.1130(02) | 0.347(4) | 5.42 | 1540 | 24640 | yes | 1.0, 1.2, 1.3, 1.4, 1.5 |
| J303 | 3.70 | 192 | 64 | 0.0662(03) | 0.262(3) | 4.24 | 531 | 8496 | yes | 1.0, 1.1, 1.2, 1.3 |
| N302 | 3.70 | 128 | 48 | 0.0891(03) | 0.353(4) | 4.28 | 1177 | 18832 | yes | 1.0, 1.1, 1.2, 1.3, 1.4 |

- $N_f = 2 + 1$ flavors of non-perturbatively improved Wilson clover fermions. [JHEP 1502 \(2015\) 043](#)
- Lüscher-Weisz gauge action [Commun.Math.Phys. 97 \(1985\)](#)
- Exceptional configurations are suppressed by a twisted mass regulator. [PoS LATTICE2008 \(2008\) 049](#)
- Generated with open boundary conditions in time. [Comput. Phys. Commun. 184 \(2013\)](#)
- Up to five source-sink separations; typically 1.0fm to 1.4fm.

Renormalization

Non-perturbative renormalization has been performed for the **three lower values of β** using the Rome-Southampton method:

| β | Z_A | $\overline{Z}_S^{\overline{\text{MS}}}$ | $\overline{Z}_T^{\overline{\text{MS}}}$ | $\overline{Z}_{v2a}^{\overline{\text{MS}}}$ | $\overline{Z}_{v2b}^{\overline{\text{MS}}}$ | $\overline{Z}_{r2a}^{\overline{\text{MS}}}$ | $\overline{Z}_{r2b}^{\overline{\text{MS}}}$ | $\overline{Z}_{h1a}^{\overline{\text{MS}}}$ | $\overline{Z}_{h1b}^{\overline{\text{MS}}}$ |
|---------|-------------|---|---|---|---|---|---|---|---|
| 3.40 | 0.75328(21) | 0.6506(19) | 0.83359(12) | 1.10492(7) | 1.11662(6) | 1.09696(7) | 1.13422(07) | 1.13805(7) | 1.14732(07) |
| 3.46 | 0.76043(17) | 0.6290(17) | 0.84754(08) | 1.12233(4) | 1.12868(4) | 1.11514(4) | 1.14753(04) | 1.15746(4) | 1.16673(04) |
| 3.55 | 0.77060(14) | 0.6129(14) | 0.86656(07) | 1.15690(4) | 1.16072(4) | 1.15014(5) | 1.17916(05) | 1.19552(5) | 1.20471(05) |
| 3.70 | 0.78788(18) | 0.5758(16) | 0.89943(12) | 1.21051(8) | 1.20719(7) | 1.20472(9) | 1.22591(10) | 1.25457(9) | 1.26365(10) |

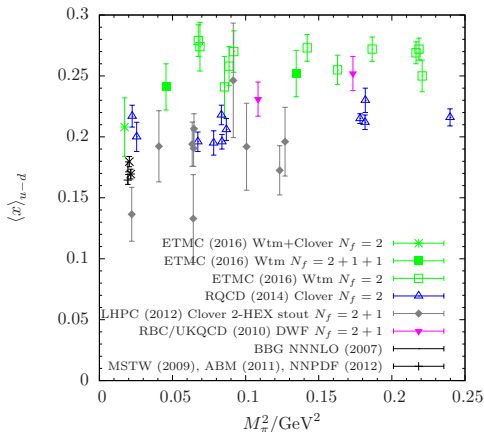
- Each of the derivative operators falls into two different irreps of $H(4)$.
- Matrix elements agree in the continuum limit.
- Blue irreps are required for the vD , aD and tD operators used in our calculation.
- Values at $\beta = 3.70$ extrapolated.
- (Relative) effects of renormalization are of similar size as found in other studies.
- Errors are statistical only; irrelevant for total error budget.
- Results are given in $\overline{\text{MS}}$ at $Q^2 = 4 \text{ GeV}^2$.

Phys. Rev. D54 (1996) 5705
Phys. Rev. D82 (2010) 114511

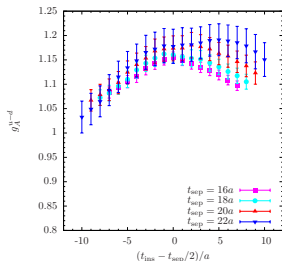
Excited states

Nucleon structure calculations are notoriously hampered by **excited state contaminations**:

- Need large t_{sep} for plateau method → **signal-to-noise problem**
- Almost all lattice determinations of g_A approach experimental value from below (at few percent level).
- Situation more severe for less well-known observables, e.g. $\langle x \rangle_{u-d}$
- Very different systematics
- Several results at physical quark masses, but chiral + continuum extrapolation unclear
- Lattice seems to favor larger values for $\langle x \rangle_{u-d}$...

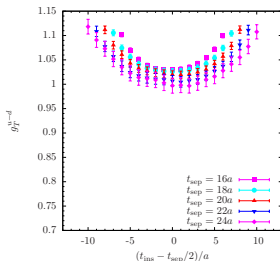


Excited states



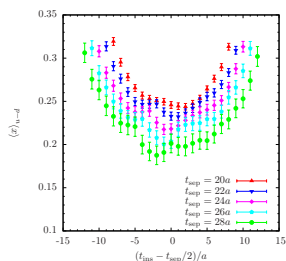
g_A on D200

($M_\pi = 203$ MeV, $a = 0.064$ fm)



g_T on N203

($M_\pi = 347$ MeV, $a = 0.064$ fm)



$\langle x \rangle_{u-d}$ on N302

($M_\pi = 353$ MeV, $a = 0.049$ fm)

- We observe excited state contamination on all ensembles.
- Contamination generally worse for twist-2 (and at smaller pion masses).
- No ground state convergence observed up to $t_{sep} = 1.5$ fm.

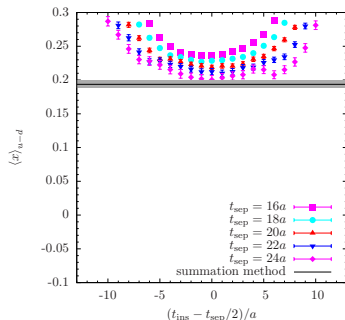
Summation method

Straightforward approach to reduce excited state-contamination

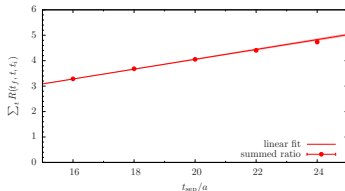
$$\sum_{t=t_i+2}^{t_f-2} R(t_f, t, t_i) \sim c + t_f \cdot \mathcal{M}_0 + \mathcal{O}\left(e^{-\Delta E(t_f-t_i)}\right)$$

Nucl. Phys. B293 (1987) 420

- Only linear fit required to obtain \mathcal{M}_0 .
- Leading excited state more strongly suppressed by $t_{\text{sep}} = t_f - t_i$
- But **large errors**
- Typically dominated by smallest t_{sep}
- Useful as Xcheck.



Plateaux and summation method on N203 ($V = 128 \times 48^3$, $M_\pi = 345$ MeV, $a = 0.064$ fm)



Linear fit for summation method on N203

Generalized pencil-of-functions (GPOF)

Instead of extending the actual operator basis, make use of the fact that

$$\mathcal{O}_{\Delta t}(t) \equiv \mathcal{O}(t + \Delta t) = \exp(H\Delta t)\mathcal{O}(t)\exp(-H\Delta t), \quad (11)$$

is a new, and **linearly independent** interpolating operator. AIP Conf.Proc. 1374 (2011)

For 2pt functions construct $(n+1) \times (n+1)$ correlation function matrix for fixed Δt , $t \equiv t_f - t_i$:

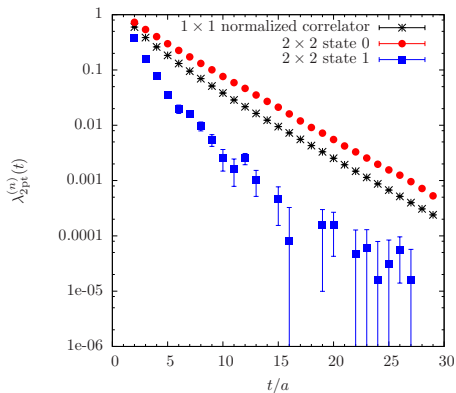
$$\mathcal{C}_{2\text{pt}}(\mathbf{t}) = \begin{pmatrix} \langle \mathcal{O}_{0,\Delta t}(t_f)\mathcal{O}^\dagger(t_i) \rangle & \dots & \langle \mathcal{O}_{0,\Delta t}(t_f)\mathcal{O}^\dagger_{n,\Delta t}(t_i) \rangle \\ \vdots & \ddots & \vdots \\ \langle \mathcal{O}_{n,\Delta t}(t_f)\mathcal{O}^\dagger(t_i) \rangle & \dots & \langle \mathcal{O}_{n,\Delta t}(t_f)\mathcal{O}^\dagger_{n,\Delta t}(t_i) \rangle \end{pmatrix} = \begin{pmatrix} C_{2\text{pt}}(t) & \dots & C_{2\text{pt}}(t+n\cdot\Delta t) \\ \vdots & \ddots & \vdots \\ C_{2\text{pt}}(t+n\cdot\Delta t) & \dots & C_{2\text{pt}}(t+2n\cdot\Delta t) \end{pmatrix}. \quad (12)$$

→ GEVP gives eigenvalues $\lambda^{(n)}(t, t_0)$ and **matrix of eigenvectors** $\mathbf{V} \equiv (\vec{v}^0(t, t_0), \dots, \vec{v}^n(t, t_0))$.

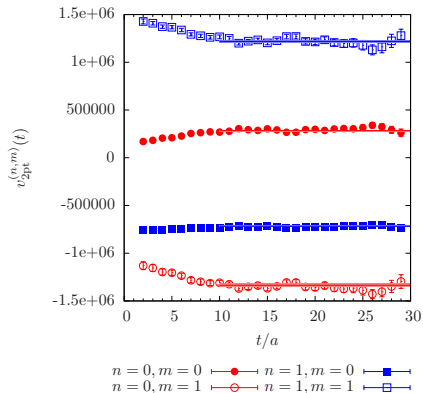
Similarly, for 3pt functions:

$$\mathcal{C}_{3\text{pt}}(t_f, \mathbf{t}, t_i) = \begin{pmatrix} C(t_f, t, t_i) & \dots & C(t_f+n\cdot\Delta t, t+n\cdot\Delta t, t_i) \\ \vdots & \ddots & \vdots \\ C(t_f+n\cdot\Delta t, t, t_i) & \dots & C(t_f+2n\cdot\Delta t, t+n\cdot\Delta t, t_i) \end{pmatrix}. \quad (13)$$

→ **This matrix is not symmetric but can be diagonalized using \mathbf{V} from 2pt case.**



Eigenvalues and eigenvectors for J303 ($V = 192 \times 64^3$, $M_\pi = 262$ MeV, $a = 0.049$ fm)



- Clear reduction of excited states for **ground state principal correlator** from 2×2 GEVP.
- Stat. err. on nucleon mass reduced by $\mathcal{O}(50\%)$.
- Some residual excited state effects remains (as expected).
- Fits to eigenvectors are stable; typically $\chi_{\text{red}}^2 \approx 1$.
- Actual choice of fit range has little impact on final result.

General procedure (sample-wise):

- 1 Solve GEVP for corresponding 2pt problem.
- 2 Fit eigenvectors in plateau region $\rightarrow V$ (time-independent)
- 3 Diagonalize $C_{3\text{pt}}(t_f, t, t_i)$:

$$C_{3\text{pt}}(t_f, t, t_i) \rightarrow V^T C_{3\text{pt}}(t_f, t, t_i) V \equiv \Lambda_{3\text{pt}}(t_f, t, t_i) = \text{diag}(\Lambda^{(0)}, \dots, \Lambda^{(n)})(t_f, t, t_i). \quad (14)$$

- 4 Replace "standard" ratio by new, optimized ratio

$$\frac{C_{3\text{pt}}(\vec{q} = 0, t_f, t_i, t; \Gamma_z)}{C_{2\text{pt}}(\vec{q} = 0, t_f - t_i; \Gamma_0)} \rightarrow \frac{\Lambda_{3\text{pt}}^{(0)}(\vec{q} = 0, t_f, t_i, t; \Gamma_z)}{\lambda_{2\text{pt}}^{(0)}(\vec{q} = 0, t_f - t_i; \Gamma_0)}. \quad (15)$$

- 5 Proceed with remaining analysis in the usual way...

Advantages:

- Method is straightforward to implement and does not require model assumptions.
- Uses existing data.
- Errors usually smaller than summation method.

A few restrictions in practice:

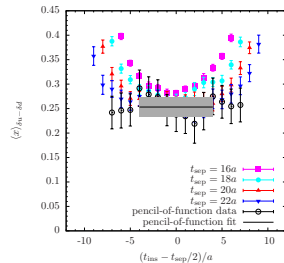
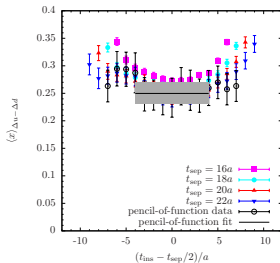
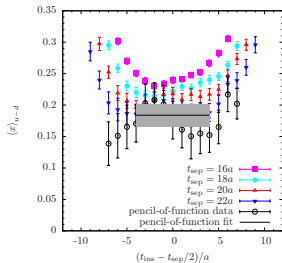
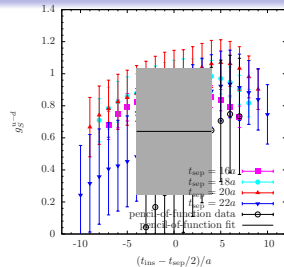
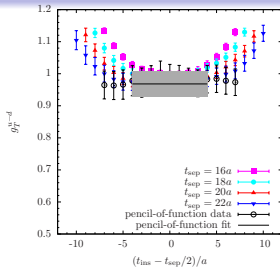
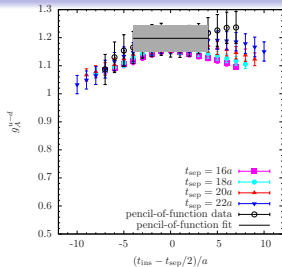
- We always have $t_i = 0$ and three up to five values for t_f .
- Need $n + 1$ equidistant values of $t_f - t_i$ to build an $n \times n$ 3pt function matrix.

⇒ We are mostly restricted to 2×2 problems.

- t_f values are spaced by $\Delta t = 2a$ (e.g. $t_f/a = 16, 18, 20, \dots$).

⇒ We are mostly restricted to $\Delta t = 2a$ in the operator construction for the 3pt case.

- Excited state removal not expected to be perfect for 2×2 GPOF
- For too many operators GPOF tends to become degenerate / singular



- GPOF results from the three largest values of t_{sep} on D200 ($M_\pi = 203\text{MeV}$, $a = 0.064\text{ fm}$)
- On average smaller errors than summation method, even for using largest values of t_{sep}
- Data points highly correlated!

(Simultaneous) Multi-state fits

The effective charge / formfactor $R^{\mathcal{O}}(t_f, t, t_i, Q^2)$ can be described by a tower of states ($t_i = 0$)

$$R^{\mathcal{O}}(t_f, t, Q^2) = G_{\mathcal{O}}(Q^2) + \sum_n \left(a_n^{\mathcal{O}}(Q^2) e^{-\Delta_n t} + b_n^{\mathcal{O}}(Q^2) e^{-\Delta'_n(t_f - t)} + c_n^{\mathcal{O}}(Q^2) e^{-\Delta'_k t_f - (\Delta_k - \Delta'_k)t} \right). \quad (16)$$

- $G_{\mathcal{O}}(Q^2)$ denotes the actual form factor,
- Δ_n, Δ'_n are energy gaps,
- $a_n^{\mathcal{O}}(Q^2), b_n^{\mathcal{O}}(Q^2)$ and $c_n^{\mathcal{O}}(Q^2)$ denote amplitudes.

Assuming symmetric plateaux for $Q^2 = 0$ we have ($g_{\mathcal{O}} \equiv G_{\mathcal{O}}(0)$)

$$R^{\mathcal{O}}(t_f, t, 0) = g_{\mathcal{O}} + \sum_n A_n^{\mathcal{O}} \left(e^{-\Delta_n t} + e^{-\Delta_n(t_f - t)} \right) + C_n^{\mathcal{O}} e^{-\Delta_n t_f}. \quad (17)$$

- $A_n^{\mathcal{O}} \equiv a_n^{\mathcal{O}}(0) = b_n^{\mathcal{O}}(0), C_n^{\mathcal{O}} \equiv c_n^{\mathcal{O}}(0)$ depend on observable \mathcal{O} .
- Δ_n are the same for different \mathcal{O} . → **simultaneous fits**
- Δ_0 is either fixed to lowest non-interacting level $2M_{\pi}$ or fitted from data.

Fit models

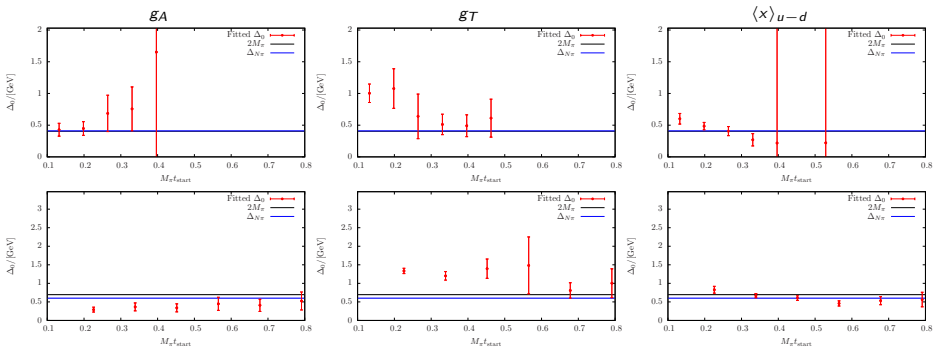
We investigated four different fit models:

- ① Simultaneous fit to all observables; first gap fixed $\Delta_0 = 2M_\pi$, second gap free (“FIT1”)
- ② **Simultaneous fit to all observables; one free gap (“FIT2”)**
- ③ Fit to individual observables; one free gap (“FIT3”)
- ④ Fit to individual observables; one fixed gap $\Delta_0 = 2M_\pi$ (“FIT4”)

Fits are subject to the following procedures / constraints:

- Data are explicitly symmetrized around $(t_f - t_i)/2 = t_f/2$.
- Fits use data from range $[t_{\text{start}}, t_f/2]$ for all available values of t_f .
- “Simultaneous” fits use local and twist-2 data **if available**, otherwise the three local charges
- **Final results from fits with same, fixed $M_\pi t_{\text{start}}$ for ALL ensembles.**
- **Can track convergence of free gap as function of $M_\pi t_{\text{start}}$ → choice for fixing $M_\pi t_{\text{start}}$.**

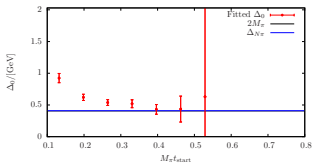
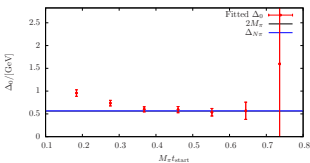
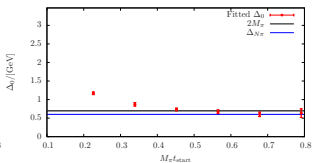
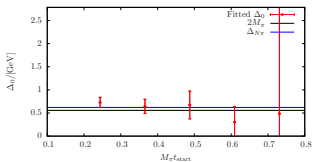
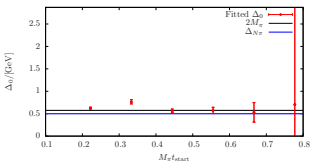
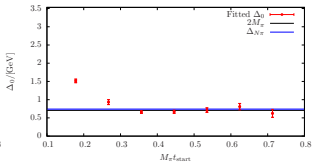
Gap convergence for single observable fits (FIT3)



Upper row: D200 ($M_\pi = 203$ MeV, $a = 0.064$ fm), lower row: N203 ($M_\pi = 347$ MeV, $a = 0.064$ fm)

- Results from fitting $R^O(t_f, t, 0) = g_O + \sum_n A_n^O (e^{-\Delta_n t} + e^{-\Delta_n(t_f-t)})$ (one parameter less; term $\sim e^{-\Delta_n t_f}$ subleading).
- Signal for Δ_0 seems to approach $2M_\pi$, but often with large errors, unstable fits.
- Not yet useful for choosing global $M_\pi t_{\text{start}}$ independent of observable, ensemble ...

Gap convergence for simultaneous fits (FIT2)

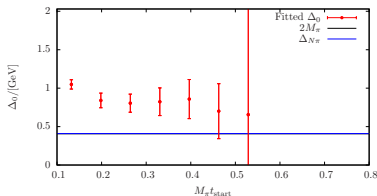
D200 ($M_\pi = 203$ MeV, $a = 0.064$ fm)N200 ($M_\pi = 283$ MeV, $a = 0.064$ fm)N203 ($M_\pi = 347$ MeV, $a = 0.064$ fm)H105 ($M_\pi = 278$ MeV, $a = 0.086$ fm)N401 ($M_\pi = 283$ MeV, $a = 0.076$ fm)N302 ($M_\pi = 353$ MeV, $a = 0.049$ fm)

- Much more precise results for Δ_0 from simultaneous fits!
- Clear convergence on most ensembles; no observable dependence.
- Trade-off between statistical error and systematics due to excited states

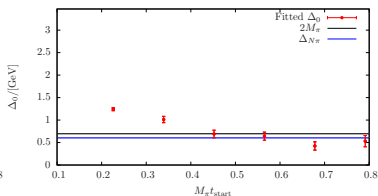
→ We choose $M_\pi t_{\text{start}} = 0.4$ for our final analysis.

Gap convergence for simultaneous fits (FIT2)

Adding term $\sim e^{-\Delta_n t_f}$ gaps become more noisy again (additional parameter):

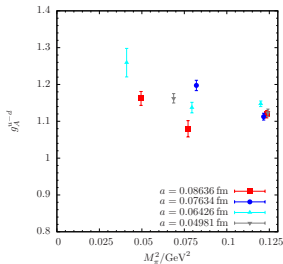


D200 ($M_\pi = 203$ MeV, $a = 0.064$ fm)

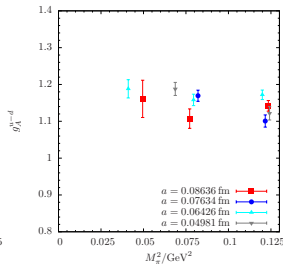


N203 ($M_\pi = 347$ MeV, $a = 0.064$ fm)

However, term $\sim e^{-\Delta_n t_f}$ not irrelevant:

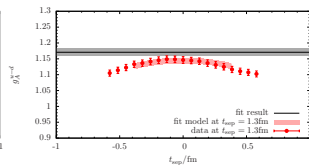
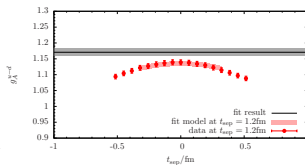
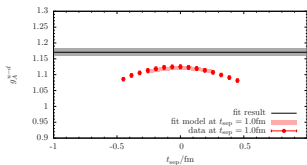


w/o term $\sim e^{-\Delta_n t_f}$

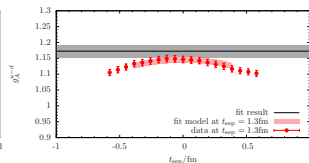
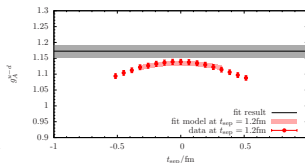
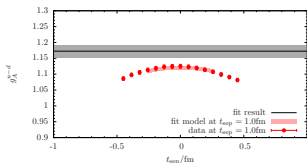


with term $\sim e^{-\Delta_n t_f}$

Fixed gap vs. free gap fit



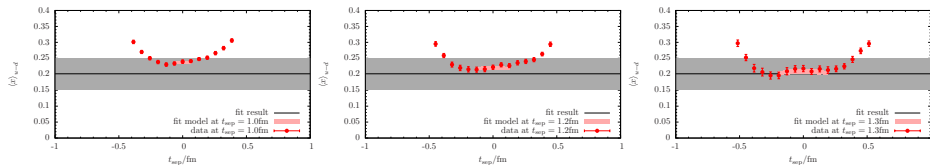
Fixed Δ_0 fit (FIT4) for g_A on N203 ($M_\pi = 347$ MeV, $a = 0.064$ fm) for three (out of five) values of t_{sep}



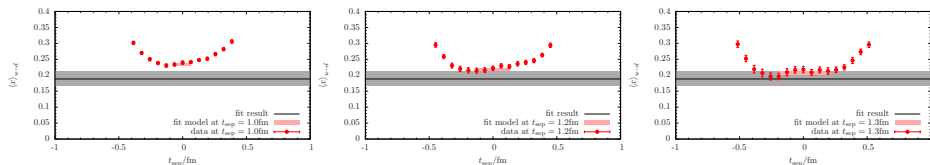
Free Δ_0 fit (FIT3) for g_A on N203 ($M_\pi = 347$ MeV, $a = 0.064$ fm) for three (out of five) values of t_{sep}

- Fits are always simultaneous for ALL values of t_{sep} !
- High statistics ensemble for testing; heavy pion mass.
- Data well described by fit form (at chosen fit range).
- Final value agrees, but larger error for free Δ_0 (as expected).
- Single observable, free Δ_0 fits are often unstable for lower statistics / fitting few points.

Fixed gap vs. simultaneous (free gap) fit



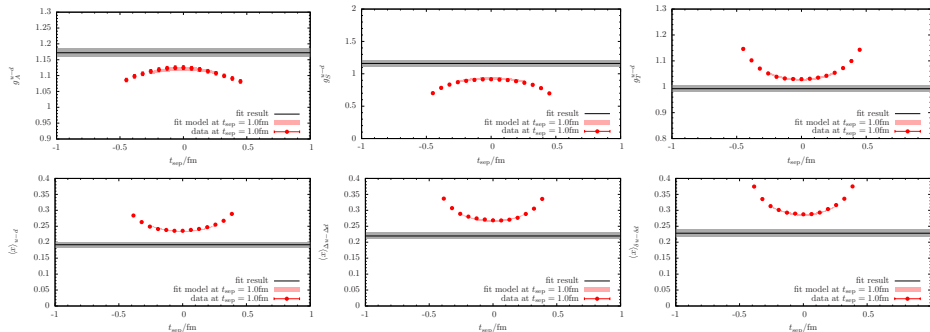
Fixed Δ_0 fit (FIT4) for $\langle x \rangle_{U-d}$ on D200 ($M_\pi = 203 \text{ MeV}$, $a = 0.064 \text{ fm}$) for three (out of four) values of t_{sep}



Simultaneous (free Δ_0) fit (FIT2). Results for $\langle x \rangle_{U-d}$ on D200 ($M_\pi = 203 \text{ MeV}$, $a = 0.064 \text{ fm}$)

- Fitting observables simultaneously results in much smaller errors.
- Often outperforms even fit with fixed Δ_0 . (!)
- Much more stable than corresponding single observable fits.

Simultaneous fit results

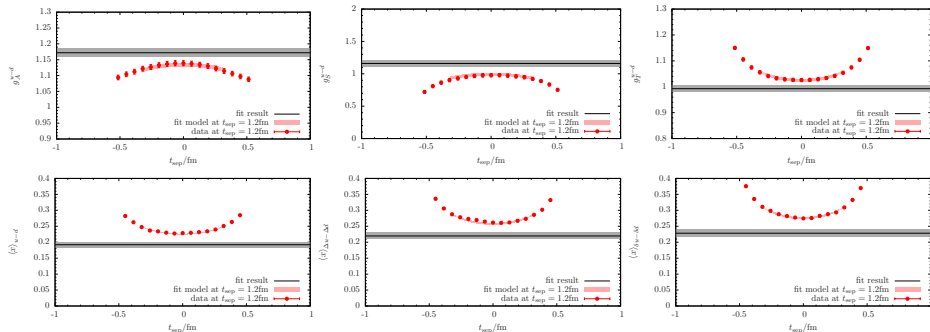


Results for all six observables from simultaneous (free Δ_0) fit on N203 ($M_\pi = 347 \text{ MeV}$, $a = 0.064 \text{ fm}$).

Results for $t_{\text{sep}} = 16a$ are shown.

- Simultaneous fits describe data very well.
- Corrections can be sizable compared to plateau method at e.g. $t_{\text{sep}} = 1.3 \text{ fm}$
- Simultaneous fits supersede fixed gap / single observable fits (less ambiguity, better signal).

Simultaneous fit results

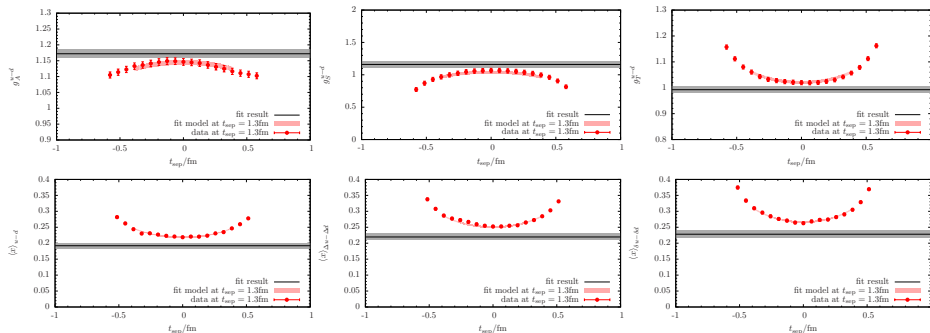


Results for all six observables from simultaneous (free Δ_0) fit on N203 ($M_\pi = 347$ MeV, $a = 0.064$ fm).

Results for $t_{\text{sep}} = 18a$ are shown.

- Simultaneous fits describe data very well.
- Corrections can be sizable compared to plateau method at e.g. $t_{\text{sep}} = 1.3$ fm
- Simultaneous fits supersede fixed gap / single observable fits (less ambiguity, better signal).

Simultaneous fit results

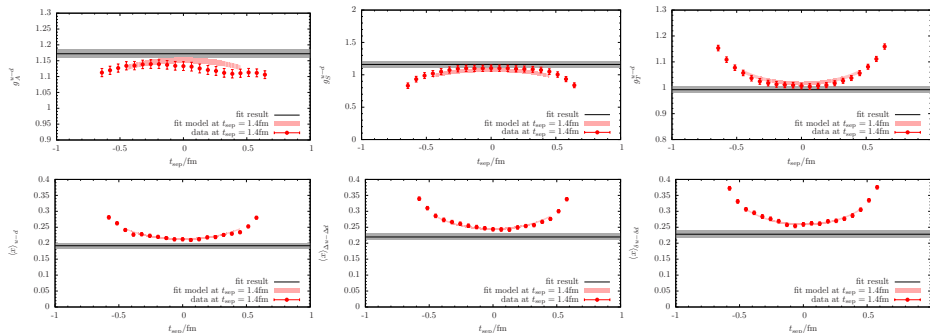


Results for all six observables from simultaneous (free Δ_0) fit on N203 ($M_\pi = 347$ MeV, $a = 0.064$ fm).

Results for $t_{\text{sep}} = 20a$ are shown.

- Simultaneous fits describe data very well.
- Corrections can be sizable compared to plateau method at e.g. $t_{\text{sep}} = 1.3\text{fm}$
- Simultaneous fits supersede fixed gap / single observable fits (less ambiguity, better signal).

Simultaneous fit results

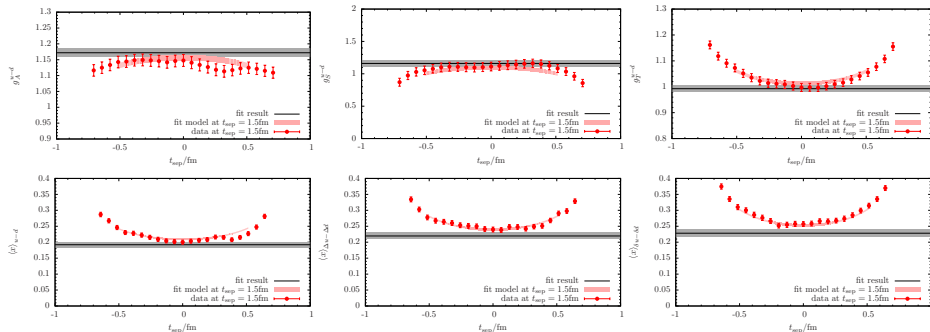


Results for all six observables from simultaneous (free Δ_0) fit on N203 ($M_\pi = 347$ MeV, $a = 0.064$ fm).

Results for $t_{\text{sep}} = 22a$ are shown.

- Simultaneous fits describe data very well.
- Corrections can be sizable compared to plateau method at e.g. $t_{\text{sep}} = 1.3\text{fm}$
- Simultaneous fits supersede fixed gap / single observable fits (less ambiguity, better signal).

Simultaneous fit results

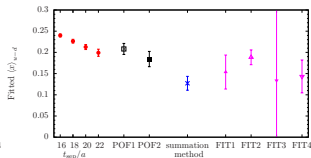
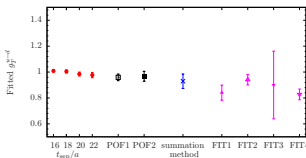
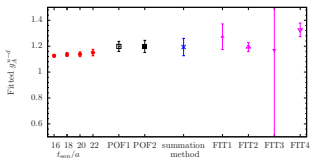


Results for all six observables from simultaneous (free Δ_0) fit on N203 ($M_\pi = 347 \text{ MeV}$, $a = 0.064 \text{ fm}$).

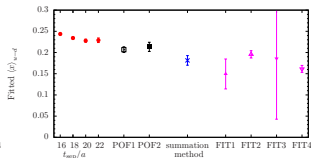
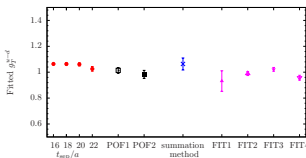
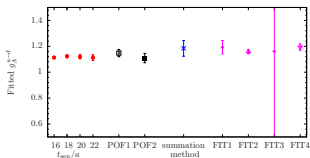
Results for $t_{\text{sep}} = 24a$ are shown.

- Simultaneous fits describe data very well.
- Corrections can be sizable compared to plateau method at e.g. $t_{\text{sep}} = 1.3 \text{ fm}$
- Simultaneous fits supersede fixed gap / single observable fits (less ambiguity, better signal).

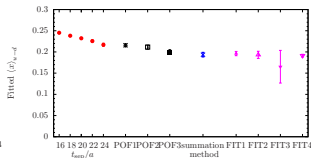
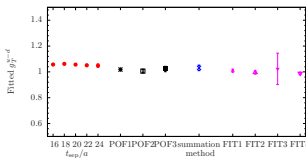
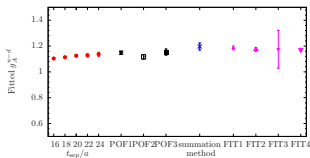
Overview of results from different methods



D200 ($M_\pi = 203 \text{ MeV}$, $a = 0.064 \text{ fm}$)

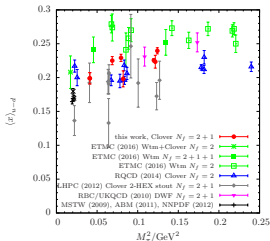


N200 ($M_\pi = 278 \text{ MeV}$, $a = 0.064 \text{ fm}$)

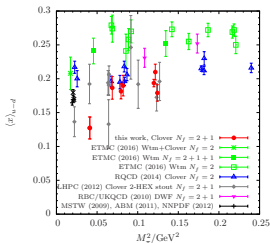


N203 ($M_\pi = 347 \text{ MeV}$, $a = 0.064 \text{ fm}$)

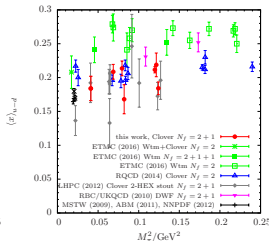
Overview of results for $\langle x \rangle_{u-d}$



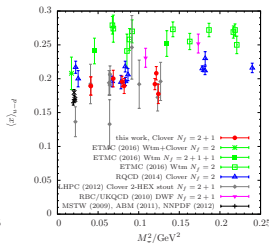
plateau method



summation method



GPOF

simultaneous fit
(all observables)

- Plateau method ($t_{\text{sep}} \gtrsim 1.4\text{fm}$) small errors and large values, as expected.
- GPOF systematically below plateau method, but non-negligible excited state contamination.
- Summation method compatible with simultaneous fit, but larger errors, unstable for most chiral ensemble.
- Results from simultaneous fit have smaller error, data less scattered than GPOF

Summary of methods

1 Plateau method

- Smallest stat. error; **non-negligible excited state contamination even for $t_{\text{sep}} \gtrsim 1.4\text{fm}$.**

2 Summation method

- Mostly compatible with fits, but large stat. errors.

3 GPOF

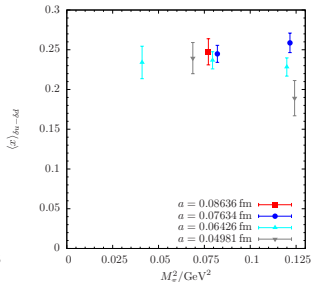
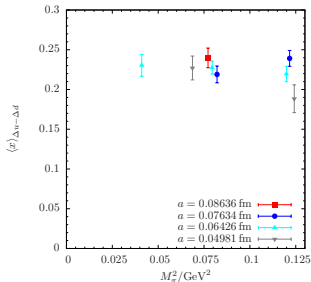
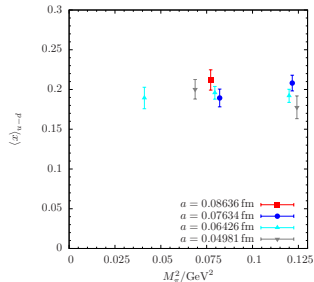
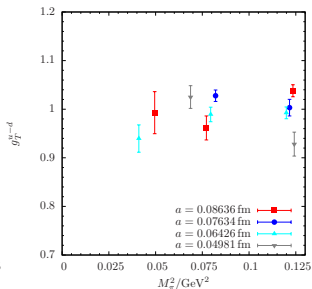
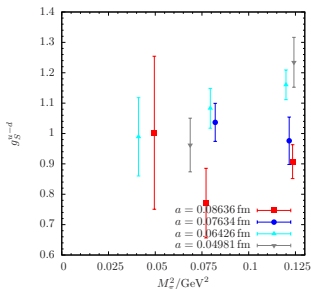
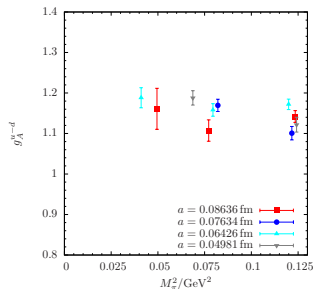
- Usually results rather close to plateau method, although systematically different.
- Larger stat. errors than plateau but smaller than summation method.
- Current setup probably not optimal; three values of t_{sep} (with larger statistics) and $\Delta t = 4a$ might be more efficient.

4 Simultaneous fits (FIT2)

- Free gap more flexible than assuming $\Delta_0 = 2M_\pi$.
- Stat. errors smaller than summation method, GPOF; more stable than other methods.
- No observable-dependent “tuning” of fit ranges, priors etc.
- **Consistent fit for all observables and all ensembles (fixing $M_\pi t_{\text{start}}$ globally).**

→ **We choose simultaneous fits (FIT2) for our final analysis...**

Raw lattice results from simultaneous fit



Chiral and continuum extrapolation

The (most general version) of our chiral and continuum fit model reads

$$O(M_\pi, a) = A_O + B_O M_\pi^2 + C_O M_\pi^2 \log M_\pi + D_O a^{n(O)}, \quad (18)$$

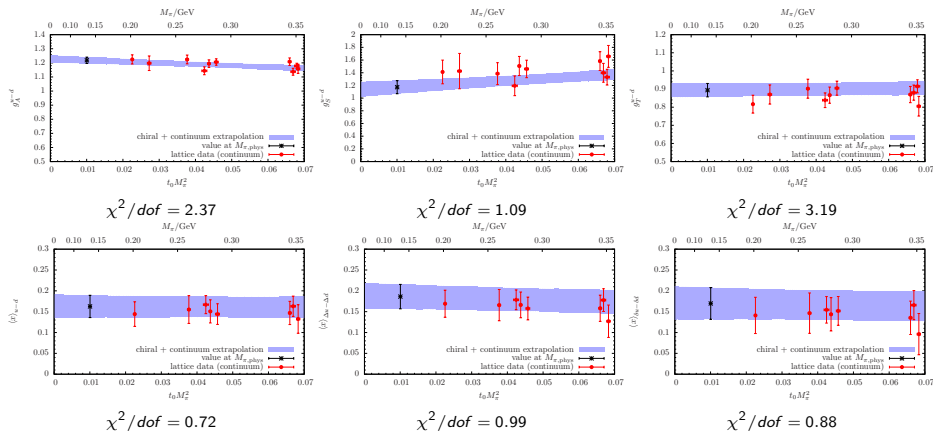
where

- $n(O) = \begin{cases} 2 & \text{if } O = g_A, g_S \\ 1 & \text{else} \end{cases}$,
- $A \equiv A_O$, $B \equiv B_O$, $C \equiv C_O$ and $D \equiv D_O$ are free fit parameters,
- For e.g. $O = g_A$ the coefficient C of the chiral log is known analytically, i.e.

$$C_{g_A} = \frac{-\dot{g}_A}{(2\pi f_\pi)^2} (1 + 2\dot{g}_A^2). \quad (19)$$

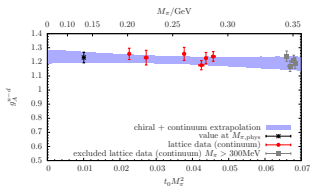
- We will denote fit models by the combination of letters used for the fit parameters of included terms, e.g. “ ABD ”.
- We find that in practice only fit models AB and ABD give reasonable results.
- Data not sensible to chiral logs, resulting in large values of χ^2/dof .
- We perform fits with and without a cut for data with $M_\pi > 290 \text{ MeV}$.

Results for model ABD, no M_π -cut

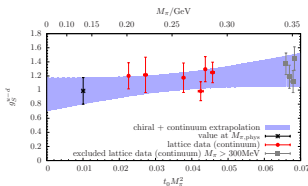


- Lattice data shown is corrected for continuum extrapolation.
- Results dominated by large ensembles with $M_\pi > 300\text{MeV}$!
- Fit to g_T and g_A do not describe data very well...

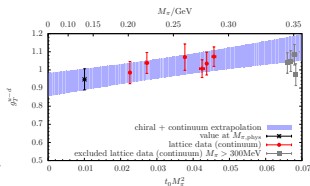
Results for model ABD, $M_\pi < 290$ MeV



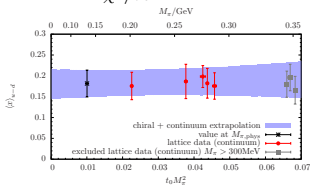
$$\chi^2/dof = 1.12$$



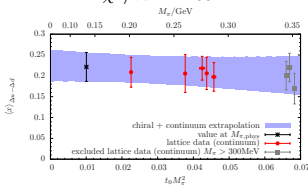
$$\chi^2/dof = 1.53$$



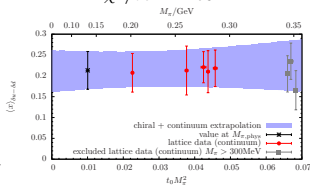
$$\chi^2/dof = 2.75$$



$$\chi^2/dof = 1.02$$



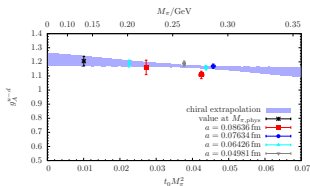
$$\chi^2/dof = 0.65$$



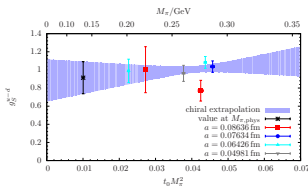
$$\chi^2/dof = 0.85$$

- Larger errors (as expected).
- Good χ^2/dof for g_A , also slightly improved for g_T .
- Chiral extrapolation very flat for twist-2 observables; but systematic shift observed.

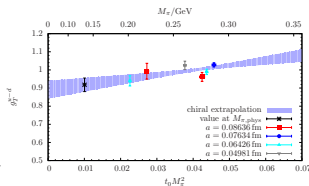
Results for model AB, $M_\pi < 290$ MeV



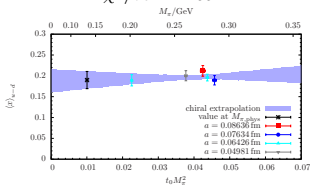
$$\chi^2 / \text{dof} = 1.55$$



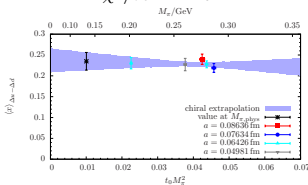
$$\chi^2 / \text{dof} = 1.47$$



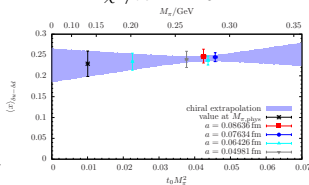
$$\chi^2 / \text{dof} = 2.18$$



$$\chi^2 / \text{dof} = 0.72$$



$$\chi^2 / \text{dof} = 0.52$$



$$\chi^2 / \text{dof} = 0.13$$

- Results without fitting term $\sim a / \sim a^2$ compatible.
- Lattice artifacts are not well resolved but still sometimes $D_0 \neq 0$ within errors!
- Fit model ABD should give more realistic errors.

Final results (still preliminary!)

Results for nucleon charges:

| Fit | g_A^{u-d} | g_S^{u-d} | g_T^{u-d} |
|------------------------|-------------|-------------|-------------|
| ABD, $M_\pi < 290$ MeV | 1.231(38) | 0.99(19) | 0.948(58) |
| ABD, all M_π | 1.218(23) | 1.17(10) | 0.894(37) |
| AB, $M_\pi < 290$ MeV | 1.205(35) | 0.91(18) | 0.918(37) |
| AB, all M_π | 1.199(18) | 0.94(09) | 0.988(18) |

Results for lowest moments of dim-4 operators:

| Fit | $\langle x \rangle_{u-d}$ | $\langle x \rangle_{\Delta u - \Delta d}$ | $\langle x \rangle_{\delta u - \delta d}$ |
|------------------------|---------------------------|---|---|
| ABD, $M_\pi < 290$ MeV | 0.182(32) | 0.221(35) | 0.213(45) |
| ABD, all M_π | 0.163(27) | 0.186(29) | 0.168(38) |
| AB, $M_\pi < 290$ MeV | 0.190(21) | 0.235(21) | 0.229(31) |
| AB, all M_π | 0.197(11) | 0.234(12) | 0.244(16) |

- Scale setting uncertainty, error on renormalization etc. propagated into stat. errors.
- Residual excited state effects should also be reflected by this error.
- g_A still somewhat smaller than experimental value.
- Result for $\langle x \rangle_{u-d}$ in good agreement with phenomenological values.

Summary and Outlook

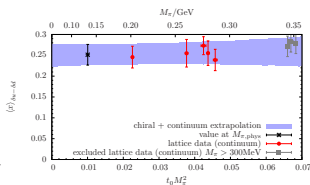
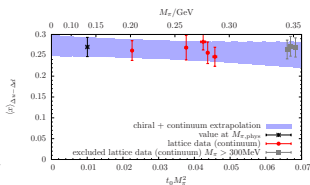
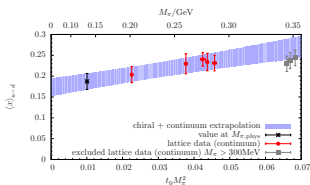
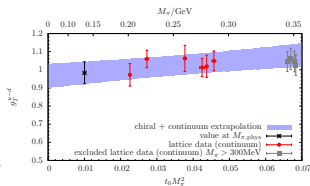
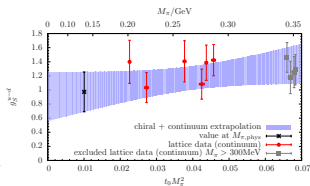
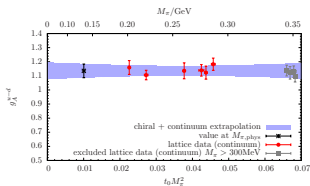
- We computed isovector charges and moments for local and twist-2 operators at four lattice spacings and for $M_\pi = 200 \dots 350$ MeV.
- We investigated several methods to deal with excited states
- Simultaneous fits promising for controlling excited states at reasonable stat. error.
- **Consistent and observable-independent analysis / treatment of excited states.**
- Large t_{sep} (and small M_π) are important.
- Combined chiral and continuum extrapolation for all observables.

Ongoing work / future plans:

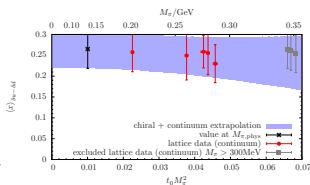
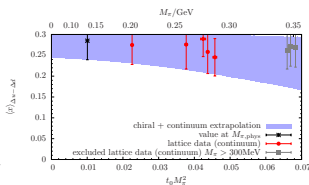
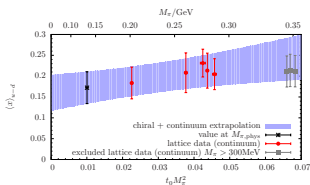
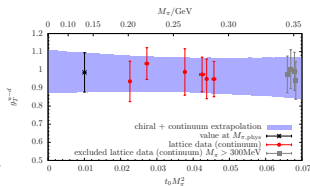
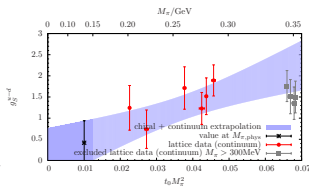
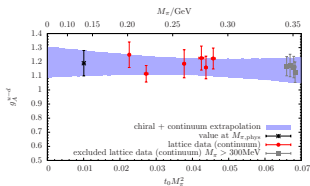
- Q^2 -dependence, e.g. el.-mag. FF, axial FF, GFFs, $\mathcal{O}(a)$ -improvement
- Inclusion of quark disconnected diagrams.
- Isoscalar observables, electro-strange FF (\rightarrow quark disconnected diagrams)
- Include ensemble $((T/a) \times (L/a))^3 = 192 \times 96^3$, $a = 0.064$ fm) at the physical point.

Backup slides

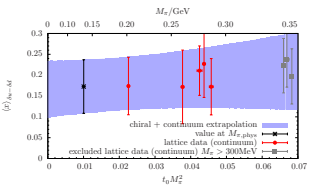
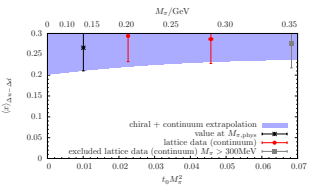
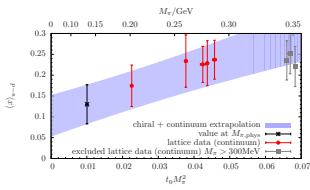
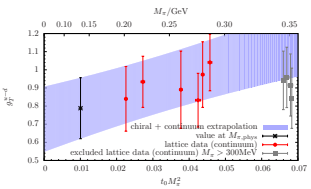
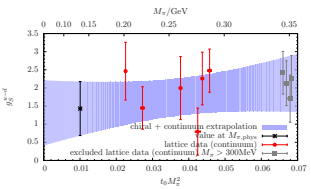
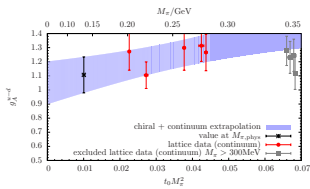
Chiral and continuum extrapolations – plateau method



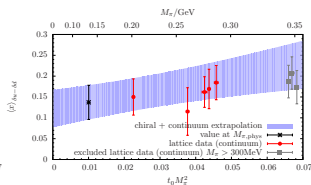
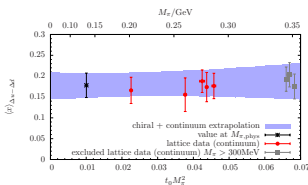
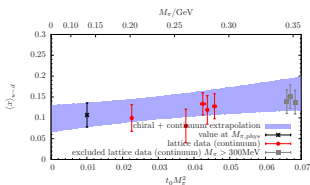
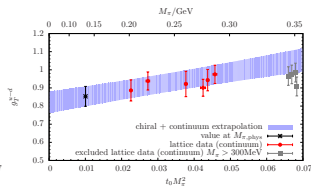
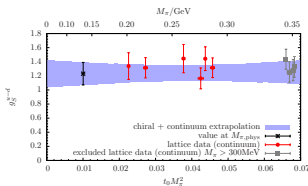
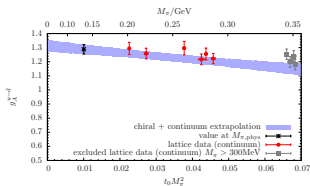
Chiral and continuum extrapolations – GPOF



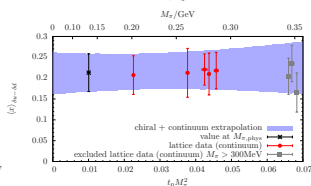
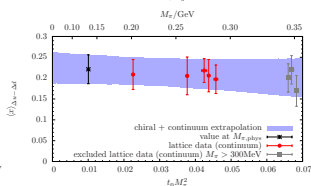
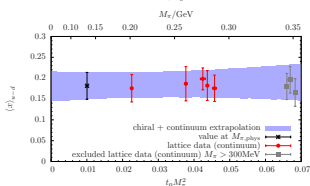
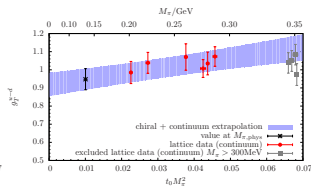
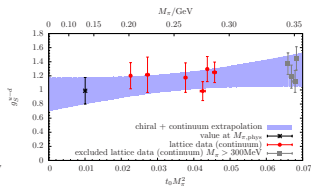
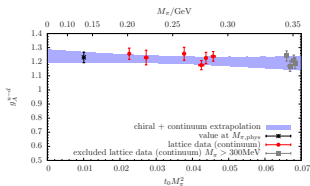
Chiral and continuum extrapolations – summation method



Chiral and continuum extrapolations – FIT2 $M_\pi t_{\text{start}} = 0.3$



Chiral and continuum extrapolations – FIT2 $M_\pi t_{\text{start}} = 0.4$



Chiral and continuum extrapolations – FIT2 $M_\pi t_{\text{start}} = 0.5$

